Application of UAV BVLOS remote sensing data for multi-faceted analysis of Antarctic ecosystem

Anna Zmarz[1*], Mirosław Rodzewicz[2], Maciej Dąbski[3], Izabela Karsznia[1], Małgorzata Korczak-Abshire[4], Katarzyna J. Chwedorzewska[4,5]

[1]*University of Warsaw, Faculty of Geography and Regional Studies, Department of Geoinformatics, Cartography and Remote Sensing, Krakowskie Przedmieście 30, 00-927 Warsaw, Poland.*

[2]*Warsaw University of Technology, Faculty of Power and Aeronautical Engineering, Institute of Aeronautics and Applied Mechanics, Nowowiejska 24, 00-665 Warsaw, Poland.*

[3]*University of Warsaw, Faculty of Geography and Regional Studies, Department of Geomorphology, Krakowskie Przedmieście 30, 00-927 Warsaw, Poland.*

[4]*Institute of Biochemistry and Biophysics, Polish Academy of Sciences, Pawińskiego 5a, 02-106 Warsaw, Poland*

[5]*Warsaw University of Life Sciences-SGGW, Department of Agreculture, Nowoursynowska 159, 02-766, Warsaw, Poland*

*corresponding author: azmarz@uw.edu.pl (A. Zmarz)
University of Warsaw,
Faculty of Geography and Regional Studies,
Department of Geoinformatics, Cartography and Remote Sensing,
Krakowskie Przedmieście 30,
00-927 Warsaw, Poland

Abstract

A photogrammetric flight was performed in December 2016 as BVLOS (Beyond Visual Line of Sight) operation over Penguin Island (South Shetland Islands, Western Antarctica). Images were taken by the PW-ZOOM fixed-wing UAV equipped with a digital SLR Canon 700D camera. The flight was performed at 550 m ASL and covered a total distance of 231.58 km. The plane take-off and landing site was near the H. Arctowski Polish Antarctic Station (Arctowski) on King George Island, South Shetlands. The main aim of the mission was to collect environmental data to estimate the size of penguin and pinniped breeding populations and to map vegetation cover and landforms. The plane returned to Arctowski with 1630 images of Penguin Island with the ground sample distance (GSD) lower than 0.07 m. The images allowed us to locate and identify individuals of two penguin species (Adélie and chinstrap), and individuals of two species of pinnipeds (Southern elephant seal and Weddell seal). Three types of tundra communities were mapped together with numerous landforms such as: volcanic, mass movement, fluvial, coastal and aeolian ones. The UAV BVLOS photogrammetric operation proved to be very robust in gathering valuable qualitative and quantitative data necessary for monitoring distant and isolated polar environments.

Key words: UAV BVLOS operation, photogrammetry, biological mapping, geomorphological mapping, South Shetland Islands, Antarctic region

Research highlights:

- UAV BVLOS operation has been successfully performed in Antarctic conditions.
- Pictured island was located over 30 km away from take-off and landing site.
- Orthophoto with a resolution of 0.07 m and DEM of 0.25 m was created.
- Precise maps of fauna, flora, and landforms of Penguin Island were drawn.
- We recommend UAV BVLOS operations for monitoring of desolate polar environments

1. Introduction

The Western Antarctic Peninsula is considered an important indicator of global climate change (Turner et al., 2009) due to the very high rates of recent environmental transformations and sensitivity of polar terrestrial ecosystems (Chwedorzewska, 2009), and therefore it focuses the attention of researchers from different fields of Earth Sciences. However, effective surveys of Antarctic environment have a lot of limitations. Small and isolated ice-free areas (oases) are frequently separated by hundreds of kilometers of natural barriers like glaciers or open sea (Convey et al., 2014). This makes systematic terrestrial surveys usually limited to small and easily accessible areas, located mainly in the vicinity of research stations with favorable topography and good microclimatic conditions where appropriate infrastructure is available (Terauds et al., 2012; Calviño-Cancela and Martín-Herrero, 2016). Due to a high cost of expeditions, logistic difficulties and very harsh environmental conditions, vast areas are still unexplored with some sites being virtually inaccessible. Such areas frequently host untouched diverse tundra communities (Androsiuk et al., 2015) and permit natural succession on landforms which undergo constant remodeling due to recent deglaciation, periglacial, coastal and sometimes volcanic processes (Zwoliński, 2007; Guglielmin, 2012). When good access to coastline is provided, such areas attract marine animals (birds and pinnipeds) which gather in huge breeding colonies (e.g. Jabłoński, 1984;

Trivelpiece et al., 1987; Salwicka and Rakusa-Suszczewski, 2002; Korczak-Abshire et al., 2012; Sierakowski et al., 2017). This combination constitutes sites of high ecological value and vulnerability to deleterious human impacts (Pfeiffer et al., 2007; Chwedorzewska and Korczak, 2010; Braun et al., 2012; Znój et al., 2017).

Remote sensing seems to be a powerful tool to detect environmental changes over difficult-to-reach terrain. Therefore, medium, high and very high-resolution satellite imagery has been used in Antarctic for ecosystem mapping and monitoring (Barber-Meyer et al., 2007; Lynch and Schwaller, 2014; Fretwell et al., 2011, 2015; McMahon et al., 2014; Pudełko et al., 2018), but its accuracy and reliability are still to be fully evaluated (Ancel et al., 2014). Satellite images proved to be especially useful in direct estimation of fauna populations (McMahon et al., 2014). To estimate the population size and trends of marine birds, mainly penguins, the images obtained from satellite (Barber-Meyer et al. 2007; Fretwell and Trathan 2009; Fretwell et al., 2012; Schwaller et al., 2013; LaRue et al., 2014; Lynch and Schwaller, 2014; Witharana and Lynch, 2016; Mustafa et al., 2017), manned aircraft, i.e. helicopters (Jabłoński, 1984; Trathan, 2004; Southwell et al., 2013) and planes (Chamaille-Jammes et al., 2000; Southwell and Emmerson, 2013) were used. However, obtaining satellite imagery material in appropriate time, according to the birds breeding chronology and in a sufficient quality is still problematic, especially in the Antarctic Peninsula region, due to frequent occurrences of dense cloud cover and mist (Mustafa et al., 2012). Manned aircraft, although commonly used in Antarctica (*after* Goebel et al., 2015; Mustafa et al., 2017; Krause et al., 2017) can gather data with a much higher resolution but their usage is limited due to lack of infrastructure, very high exploitation cost and potential intrusive influence for wildlife (Harris, 2005; Hughes et al., 2008; Watts et al., 2012; Christie et al., 2016).

Multidecadal warming and resulting geomorphic changes on South Shetland Islands (Zwoliński, 2007; Kejna et al., 2013) attract geomorphologists to map the area using

conventional aerial photography and satellite images based on visual light (López-Martínez et al., 2012) or radar radiation (Schmid et al., 2016). Fixed-wing UAV operations in geomorphic mapping are still seldom used (Dąbski at al. 2017) in the Antarctic region. Owing to the development of the autonomous controllable micro-airplanes technology, platforms intended for the task flights within the Antarctic areas (Goetzendorf-Grabowski and Rodzewicz, 2017) can be constructed, but this technology is still new in collecting environmental data in polar regions (Zhou, 2009; Watts et al., 2012; Dąbski et al., 2017) and requires further development. UAVs bridge the scale gap between field-based observations and full-scale airborne or satellite surveys (Anderson and Gaston, 2013; Berni et al., 2009; Lucieer et al., 2014). However, there are significant differences in the UAV platforms used (rotary- or fixed-wing) and the resolution of the imagery collected. The advantage of a fixed-wing UAV is that it allows us to cover significantly larger surface with high-resolution images in one flight, especially during the Beyond Visual Line Of Sight (BVLOS) surveys. Moreover, such platforms fly faster than rotary ones, thus being more resistant to strong, unpredictable Antarctic winds up to 23 ms^{-1} (Korczak-Abshire et al., 2016; Dąbski et al., 2017), and exert only a minor impact on animals (Korczak-Abshire et al., 2016) in comparison with the rotary wing platforms (Vas et al., 2015; Rümmler et al., 2016).

The aim of this study is to show methodology of our BVLOS fixed-wing UAV flight in the maritime Antarctic, and to show results of environmental data acquisition over Penguin Island located at a significant distance from the station facility (take-off and landing site). During the 2016 summer season, the UAV was deployed 12 times from the vicinity of the Henryk Arctowski Polish Antarctic Station (Arctowski) and digital data on fauna, flora, and landforms has been collected from King George Island (KGI) and its surroundings in the South Shetland Islands, maritime Antarctica (Fig. 1). The operation was conducted as part of the project "A novel approach to monitoring the impact of climate change on Antarctic

ecosystems (MONICA)". One of the flights was performed over distant Penguin Island located near the SE coast of KGI, at the entrance to King George Bay.

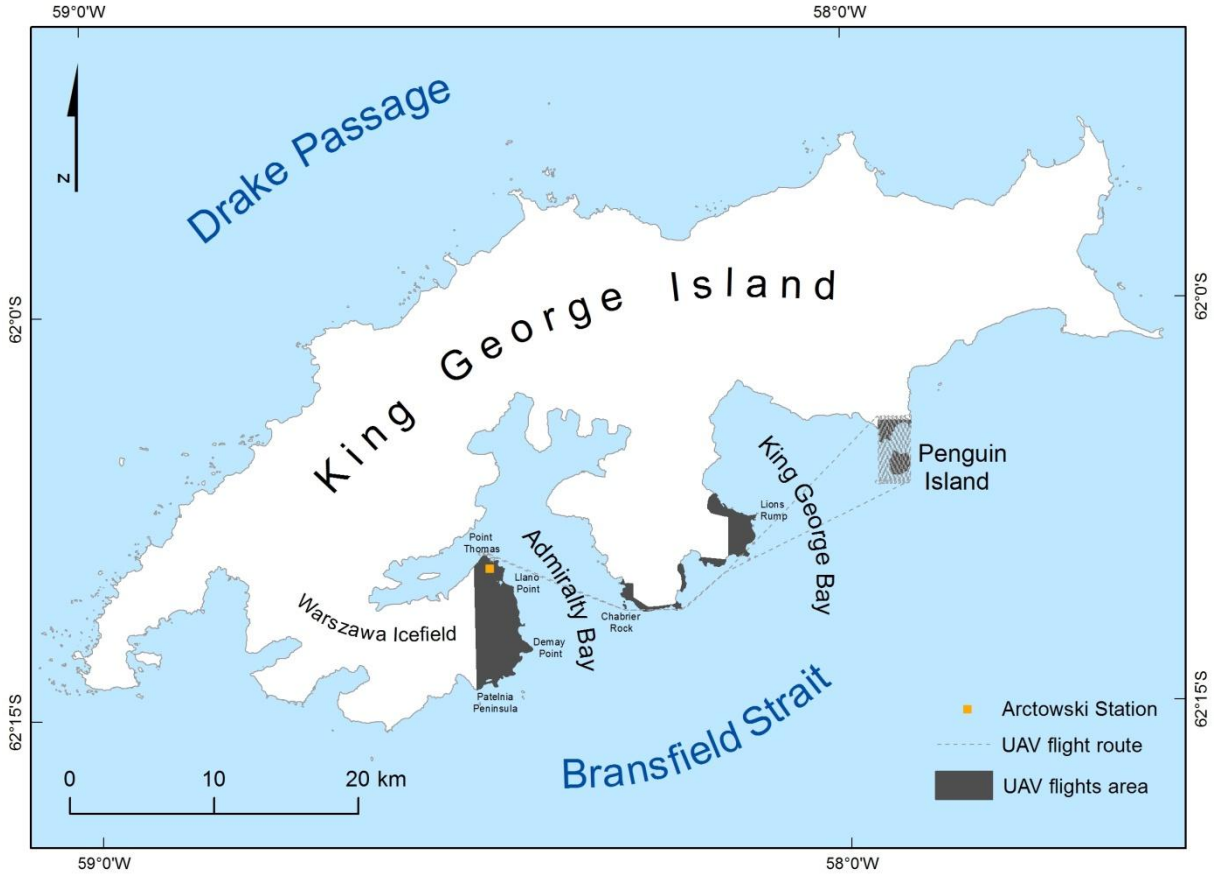

Fig. 1. Location of all photogrammetric flights performed during summer season 2016 based on Arctowski; the total area covered was 34.51km^2 (marked in dark grey). Selected UAV flight route to Penguin Island is marked in scatter line. [The coastline of the island on the basis of the SCAR King George Island geographic information system project (http://www.kgis.scar.org/)].

2. Methods

The date of flight (1 December 2016) was determined using the breeding chronology data of the investigated animal species, on the basis of each day direct ground observations in easily accessible colonies located near Arctowski. On the date of the flight, most non-breeding penguins had left, and the breeding population remaining at the site was composed

almost entirely of single adult individuals on their nests incubating eggs. Moreover, very limited snow cover in December permitted imaging of flora communities and landforms.

2.1. UAV specifications

The unmanned aerial vehicle PW-ZOOM (Fig. 2, Table 1) was designed, manufactured and tested at the Warsaw University of Technology in Poland (Goetzendorf-Grabowski and Rodzewicz, 2017; Rodzewicz et al., 2017).

Fig. 2. Unmanned Aerial Vehicle PW-ZOOM on King George Island.

The aircraft was equipped with an automatic control system (autopilot) linked with a telemetry module (Table 2). A similar module was applied in the Ground Control Station, which was connected to the computer with special software HORIZON^{mp} (MicroPilot, Stony Mountain, Canada) for planning the flight path and managing the UAV flight. In order to collect the photogrammetry data, the UAV was equipped with the system consisting of the

152 photo-camera (Table 3) linked with the GPS and the special bed for vibroisolation and impact
153 protection of the camera. A special slot in the bottom of the fuselage protected a camera lens
154 during the landings. In order to adapt the aircraft to operations in low temperatures,
155 the carburetor of the engine, and the Pitot tube (i.e. airspeed sensor) had deicing protection.
156 Also, the front of the fuselage was strengthened, which made it possible to land without
157 damaging the equipment while landing on rough surfaces (on stones or ice).

158

159 Table 1. Technical specifications of the UAV platform.

UAV TYPE	PW-ZOOM
Wingspan	3.19 m
Wing area	1.29 m^2
Wing airfoil	Eppler E-205
Engine	2-Stroke 3.58 kW (DLE40)
Propeller	19x10"
Optimal cruise speed	100 - 110 km/h
Max. speed of horizontal flight	160 km/h
Max. take-off weight	23 kg
Payload	3.5 kg
Max. operational range	160 km (330 km with the extended tank mounted instead of parachute system)
Tolerable wind speed limit	23 ms^{-1}
Autopilot	MP2128g produced by MicroPilot (Canada)
GPS	TIM-4P GPS modules
Telemetry module	YM6500, SATELLINE – EASY
Telemetry range	25 km
Fuel	95 octane gasoline /2-stroke oil 30:1 mixture

160

161 Table 2. Specification of autonomous flight equipment.

DEVICE	PARAMETERS
AUTOPILOT: MP2128g	produced by MicroPilot (Canada)
Main features:	GPS waypoint navigation with altitude and airspeed hold, fully integrated with 3-axis gyros/accelerometers, GPS, pressure altimeter, pressure airspeed sensors, extensive data logging and telemetry link.
Sensors:	4 Hz Ublox GPS receiver 5G 3-axis accelerometers gyros of 250º/sec maximum rotation rate
Ground control software:	HORIZON^{mp}

Operating temperature range:	-20°C – +65°C
Telemetry Module:	YM650 SATELLINE – EASY produced by SATEL Company, Finland
Frequency	403 – 473MHz
Carrier power	100, 200, 500, 1000 mW
Communication Mode	Half-Duplex
Input Voltage	6 – 30V/1A DC
Interface	Port 1: RS-232/Port2: RS-232/422
Data speed of Serial Interface	300 – 38400 bps
Weight	254 g (without cables and antenna)
Operational Temperature Ranges	-25°C – +50°C (ETS Standard), -40° C – +75°C (absolute min./max.)
Ground station telemetry antenna:	CA450Y+TNC (440-475MHz)
UAV telemetry antenna:	RMILEC SR771 UHF435MHz

Table 3. Type of camera used in the experiment.

CANON 700D	PARAMETERS
Image sensor	22.3 x 14.9mm CMOS
Pixels	18
Lens	35mm f / 2.0
Image	RAW, JPEG
Communication and connectors	USB 2.0 Hi-Speed (Mini-B), Output video (PAL/ NTSC), Output mini HDMI typu C (HDMI-CEC), Output RS-60E3, Remote control RC-6, Receiver GPS GP-E2
Power	LP-E8 (7.2 V, 1120 mAh)
Recorder	Secure Digital (SD/SDHC/SDXC)
Weight with the lens &battery	1200g

The range of telemetry communication depends on the power adjustment setting of the modem, as well as on the kind of antennas used in the ground station and on the plane, and also on the environmental conditions. It was empirically proved that if the power of transmission is set to 1W and there are no obstacles between the antennas, then the range of telemetry is at least 30 km. It was also checked for long-range transmission that the best option was to set the transmission speed to 4800 bps (i.e. lowest value).

2.2. Flight details

The flight was performed on 1 December 2016 by a three-person team: the remote control pilot, the ground control station operator and the technical operator. All team members had licenses to operate BVLOS flights.

The take-off and landing site was located near Arctowski, 30 km away in a straight line from Penguin Island. The take-off was carried out with the launcher, while landing was done on a small ground field near the beach (about 100 m long). The flight path was in the form of a photogrammetry grid (Fig. 3). The distance between the grid lines was 70 m (which provided 70% forward and side overlap), the length of the lines was 4100 m, and flight altitude 550 m ASL. Total distance covered during the flight was 230 km (Table 4). In order to maintain safety rules during the flight and proper telemetry, the planned altitude of the flight was determined by the ground surface features such as glacier caps, nunataks or hills. The chosen altitude of flight allowed us to obtain digital images with a ground sampling distance (GSD) of 0.07m. Flight routes were prepared in HORIZON^{mp} software.

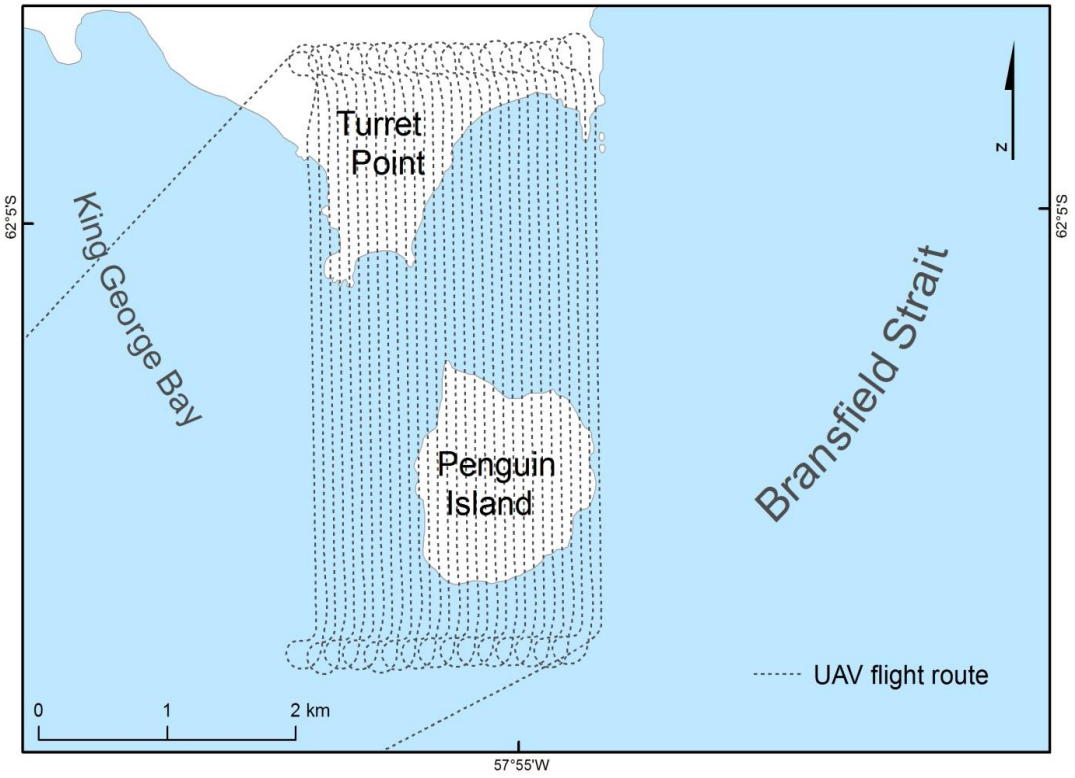

Fig. 3. Fight path above Penguin Island.

Table 4. The parameters of the aerial survey to the Penguin Island performed on 1 December 2016.

PARAMETERS	
UAV	PW-ZOOM
Distance	230 km
Cruise speed	102.6 km/h
Total time of flight	2h 14 min 30 s
Camera set	Canon 700D with 35mm lens (RGB)
Number of images	1630 (format: RAW)
GSD	0.07 m

192 **2.3.Data processing**

193 The images were obtained in RAW format during the flight and converted to JPEG
194 format in the Digital Photo Professional version 3.13.0.1 (Canon INC) software. All images
195 had georeferences (X, Y, Z) registered by the autopilot logger mounted on UAV. Images
196 showing Penguin Island were processed into an orthophoto with a resolution of 0.07 m and a
197 Digital Elevation Model (DEM) of 0.25 m resolution in the original WGS84 coordinate
198 system. The Agisoft Photoscan Professional software Version 1.3.2 build 4205, 64bit (Agisoft
199 LLC.) and Structure from Motion (SfM) algorithm were used to create the orthophoto and
200 DEM. In order to obtain data on fauna, flora, and landform, the orthophoto was converted to
201 the UTM system, zone 21S (EPSG:32721) in ESRI (Environmental Systems Research
202 Institute) ArcGIS 10.3 software.

203 Censuses of penguin breeding population size, expressed in the number of occupied
204 nests visible on the orthophoto were done in ESRI ArcGIS 10.5 software by
205 photointerpretation using gridcell-by-gridcell method (e.g. Hodgson et al., 2016). Three
206 separate counts of individuals occupying nests in each of the breeding groups in both colonies
207 identified on the orthophoto were carried out by the experienced photo interpreter. Each of the
208 results obtained differed by no more than 10%, and the mean value [$\overline{X}$] was calculated; see
209 recommendations of CCAMLR (2014), A3A and A3B standard methods for monitoring
210 parameters of predator species. “Calculate geometry” option in ESRI ArcGIS 10.5 software
211 was used for estimating the size of polygon areas occupied by the birds.

212 The range of plant communities was indentified on aerial photographs and vectorised
213 using ESRI ArcGIS 10.5 software. Photointerpretation in scale 1:300 was made by a qualified
214 person who also conducted direct ground observations in 2008/2009 Antarctic summer season
215 (Chwedorzewska unpublished data), when five dominated tundra communities were identified
216 and map.

Identification of landforms was based on previous findings of Birkenmajer (1979, 1982) and on the analysis of UAV images and DEM obtained. The landform were manually vectorised using ESRI ArcGIS 10.5 software based on careful analysis of orthophoto usually in a scale 1:800, but some cases down to 1: 100 (when vectorizing very small landforms, e.g. volcanic bombs, outcrops of bedrock, erosional furrows), DEM (at different angles and scales), and comparison with previous geological maps (Birkenmajer 1979, 1982; Pańczyk and Nawrocki, 2011), and our knowledge of typical landforms such as braided channels, creep terraces, dunes. For example, we draw flanks of Deacon Peak using manually depicted lower edifice boundary along relief concavity at foothills and manually depicted crater rim (clearly visible crest line). No specific algorithm was used. Small landforms such as fluvial channels, creep terraces or dunes could be vectorised based on a spatial arrangement of color or intensities (image texture). The smallest identified and vectorised (mapped) landform was one of the volcanic bombs, and has an area of 0.170388 m^2 in reality.

3. Study site

Penguin Island measures 1750 m N-S and 1500 m E-W and is located about 0.75 km south of King George Island, at the western entrance to King George Bay (Fig. 1). The island is under the influence of a relatively warm Bransfield Current originating from the Transitional Zonal Water with Bellingshausen Sea influence (Sangrá et al., 2011), and maritime climate conditions with air temperature frequently crossing 0°C in each month of the year, high humidity and strong winds (Rakusa-Suszczewski, 2002). The island is a resting, breeding and forage area for marine birds and pinnipeds (Jabłoński, 1980, 1984; Naveen et al., 2000; Pfeiffer and Peter, 2004; Sander et al., 2007; Korczak-Abshire et al., 2012; Harris, 2015) and it hosts scattered, dry tundra communities. The main landforms of the island are the principal cone of the Deacon Peak stratovolcano (180 m a.s.l.), situated in the SW part of the

island, and the Petrel Maar developed at the foothills of the stratovolcano near the eastern coast of the island and hosting a lake (Fig. 4). The island was formed in result of volcanic activity connected with the opening of the Bransfield Straight in the Pliocene (Birkenmajer, 1979, 1982; Pańczyk and Nawrocki, 2011).

Fig. 4. 3D view on Penguin Island from S, based on UAV images.

4. Results

Below, we present the results of detailed qualitative and quantitative UAV image and DEM analyses which focus on fauna, flora and landforms of Penguin Island.

4.1. Fauna

The high-resolution orthophoto allowed us to map eight breeding groups of Pygoscelid penguins, in two colonies situated in the northeastern (NE) and southwestern (SW) part of the island (Fig. 5). On the basis of published data (e.g. Pfeiffer and Peter, 2004, Sander et al., 2007) and own direct ground observations from previous years, it was assumed that NE breeding site consists of only one *Pygoscelis* species: chinstrap (*P. antarcticus*), while in the

SW two species: chinstrap and Adélie (*P. adeliae*) nest together. Body size of adult individual of Adélie measures 70-71 cm and chinstrap penguin 67-76 cm (Shirihai 2002), which is enough to be clearly seen on the images of spatial resolution 0.07 m. Individuals occupying nests in both colonies were identified on the orthophoto (Fig. 5A) and counted using the method described in section 2.3. In total 4,109 occupied nests of chinstrap and Adélie were identified in NE and SW parts of the island (Fig. 5, Tables 5, 6). In the case of Adélie and chinstrap penguins the internest distances for both species are comparable (43.2±1.3 cm Adélie; 59.2± 2.2 cm chinstrap) and significantly shorter than for the third *Pygoscelis* species breed in this region, gentoo (*P. papua*) (74.3±3.8 cm) (Volkman and Trivelpiece, 1981). The structure and distribution of individuals occupying nests identified in the breeding groups within analyzed orthophoto corresponds with the characteristic for preferences of two identified species (Fig. 5B, 6).

On the NE part of the Island four breeding groups of chinstrap penguins were recorded and consisted of 3,504 (SD=48.3) individuals occupying nests (Table 5). The number of chinstrap and Adélie occupied nests in mixed colony on SW coast of island was estimated at 605 (SD=19.5). These birds formed four groups and several scattered nests (Table 6).

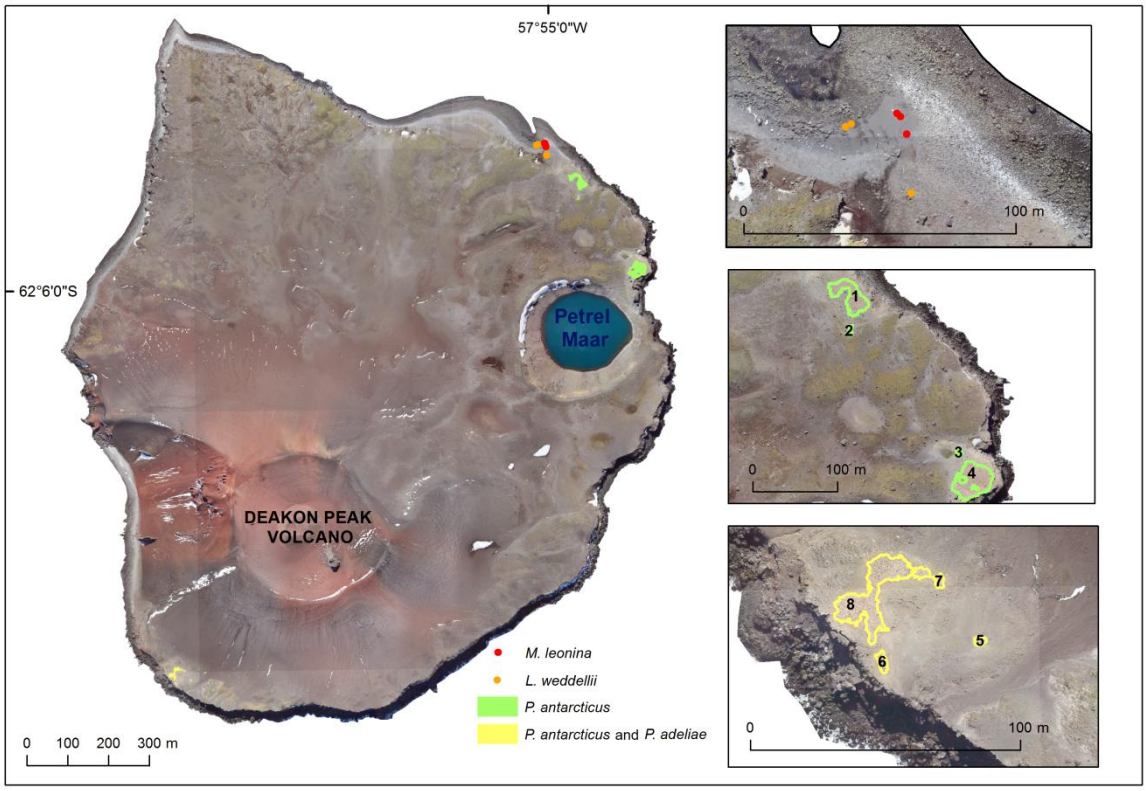

Fig. 5. Localization of investigated fauna species: pinniped individuals (*Mirounga leonina* and *Leptonychotes weddellii*), and penguin breeding colonies NE (*P. antarcticus*), SW (*P. antarcticus* and *P. adeliae*); based on UAV images (vectorised in ESRI ArcGIS). The number of breeding groups according to Table 5 and 6. The border of polygon areas occupied by the birds incubating eggs marked in green and yellow.

Additionally, 6 pinniped individuals: 3 of the southern elephant seal (*Mirounga leonina*) and 3 of the Weddell seal (*Leptonychotes weddellii*) (Fig. 5, 5A, 5B) were identified on the NE coast in the vicinity of penguin breeding colony. Species were identified based on the analysis of following traits: pelage patterns and colors, shape and size of seals in the image (see Fig 5B). Among four species of pinnipeds characteristic for the Penguin Island (Jabłoński, 1980), only these two were identified; neither crabeater seal (*Lobodon carcinophaga*) nor fur seal (*Arctocephalus gazella*) were observed, contrary to our expectations (Salwicka and Rakusa Suszczewski, 2002).

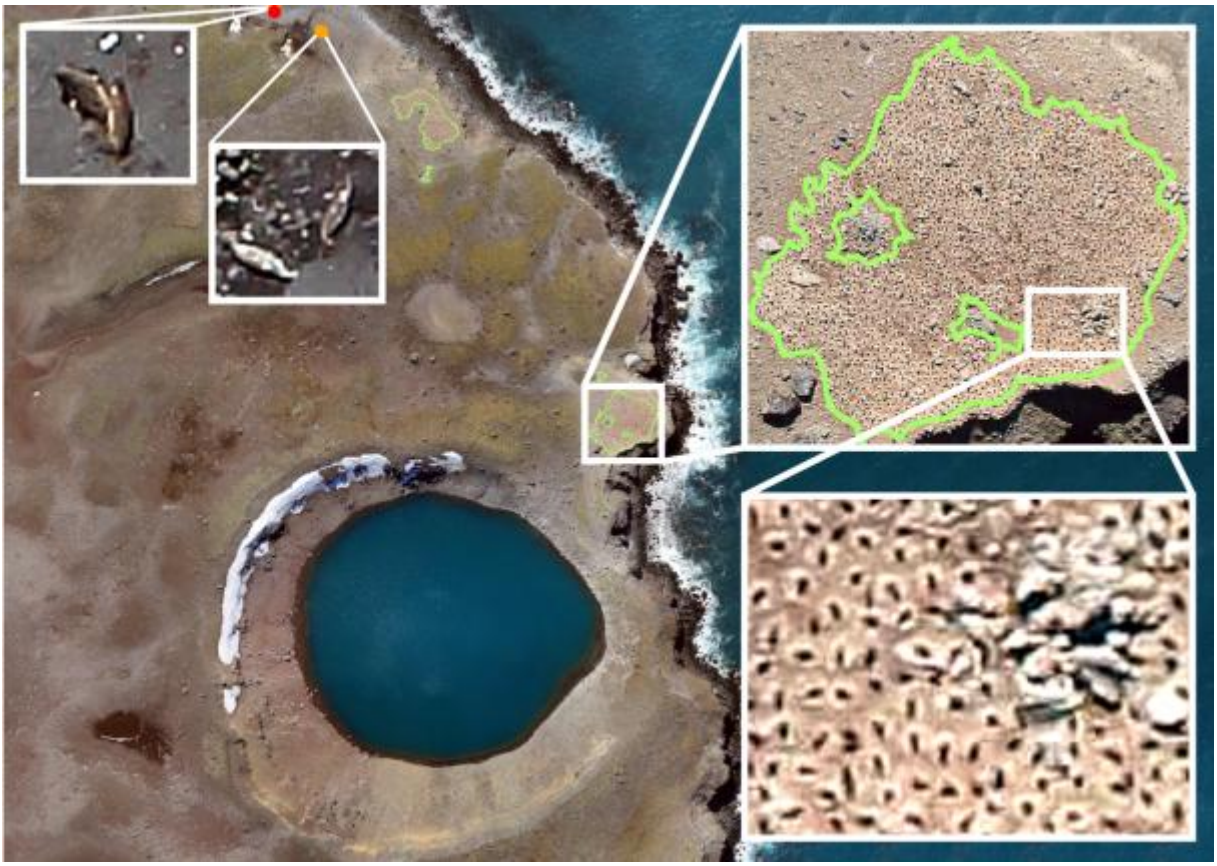

Fig. 5A. A part of analyzed orthophoto with localization of investigated fauna species: individuals of pinniped ● *M. leonina* and ● *L. weddellii*; individuals of *P. antarcticus* penguin concentrated in four breeding groups of NE colony (borders of polygons marked in green; vectorised in ESRI ArcGIS).

Table 5. Number and size of polygons identified on the orthophoto as penguin breeding groups; number of occupied nests of *P. antarcticus* identified in the colony situated on NE coast of Penguin Island.

SPECIES	GROUP No.	POLYGON SIZE [m^2]	I NEST CENSUS	II NEST CENSUS	III NEST CENSUS	AVERAGE NUMBER OF NEST [$\overline{x}$]	STANDARD DEVIATION
P. antarcticus	1	904	1346	1429	1349	1375	47.080
P. antarcticus	2	38	58	57	56	57	1.000
P. antarcticus	3	31	55	57	54	55	1.530
P. antarcticus	4	1352	2006	2015	2030	2017	12.120
TOTAL		**2325**	**3465**	**3558**	**3489**	**3504**	**48.3**

Table 6. Number and size of polygons on the orthophoto identified as penguin breeding groups; number of occupied nests of *P. antarcticus* and *P. adeliae* identified in the mixed colony situated on SW coast of Penguin Island.

SPECIES	GROUP No.	POLYGON SIZE [m^2]	I NEST CENSUS	II NEST CENSUS	III NEST CENSUS	AVERAGE NUMBER OF NESTS [$\overline{X}$]	STANDARD DEVIATION
P. antarcticus/ *P. adeliae*	5	11	24	24	24	24	0.000
P. antarcticus/ *P. adeliae*	6	20	40	34	36	37	3.060
P. antarcticus/ *P. adeliae*	7	13	17	17	18	17	0.580
P. antarcticus/ *P. adeliae*	8	341	529	508	543	527	1.762
TOTAL		**385**	**610**	**583**	**621**	**605**	**19.5**

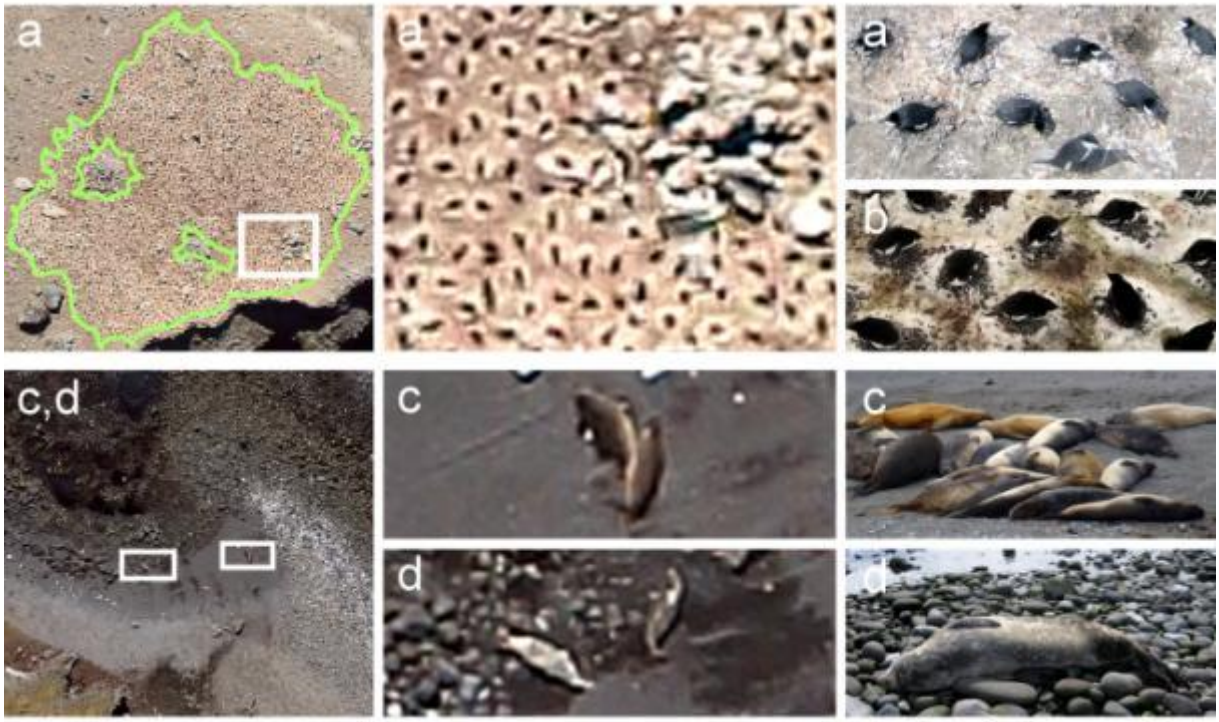

Figure 5B. Imagery of sampled colony of penguin and pinnipeds on remote Penguin Island: (a) chinstrap penguin *P. antarcticus* NE breeding group No. 4 (b) Adélie penguin *P. adeliae* (c) elephant seal *M. leonina* individuals (d) Weddell seal *L. weddellii* individuals. The main left images of analyzed orthophoto was captured by the UAV to make estimates of the number of individuals for each species. The middle inset of each panel is a magnified view of the left

311 image. Right insets illustrate the example of vantage of a ground census. The right insets are
312 not to scale (photo by M. Korczak-Abshire).
313

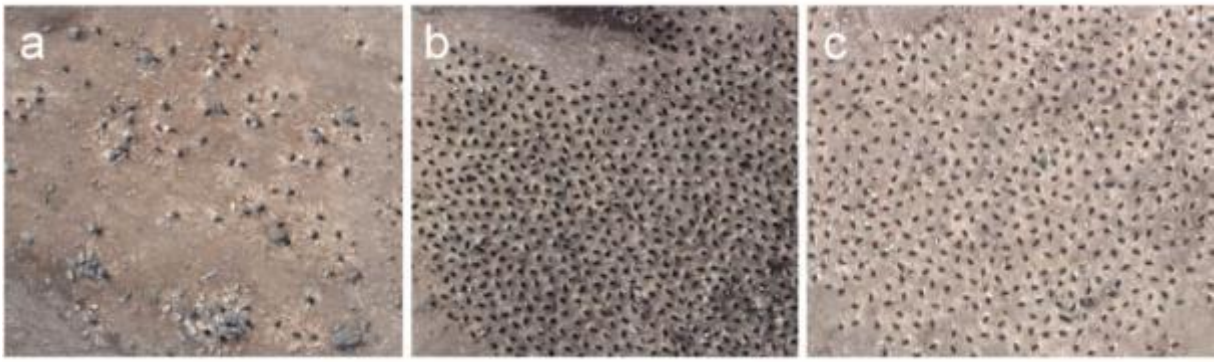

314
315 Fig 6. Example of characteristic and definite structure and distribution of individuals
316 occupying nests identified in the breeding groups of three different *Pygoscelis* penguin
317 species: a) gentoo, b) Adélie, c) chinstrap. UAV derived material, 16 Nov 2014, RGB images,
318 GSD 0.05 m (according to Zmarz et al. 2015).
319
320 **4.2. Flora**
321 On the breeding penguin colony, all the vegetation has been devastated due to
322 excessive manuring and treading down by birds. Only ornithocoprophilus lichens can be
323 recorded on stones and rocky cliffs. But in the marginal zone of penguin breeding area
324 appeared a dense cover of green algae *Prasiola crispa* (Lightfoot) Meneghini and individual
325 big tussocks of *Deschampsia antarctica* Desv. appeared at less exposed to direct contact with
326 guano sites (Fig. 7). However, shortly after the breeding season, the rookeries were colonized
327 by *P. crispa*, which can rapidly develop extensive mats covering the whole area, thus this
328 community can be easily identified from images.
329 The south and central parts of the Deacon Peak are almost devoid of vegetation, due to
330 steep slopes covered by loose and unstable substratum (Fig. 7). The north flat, windswept part
331 of the island with limited access to nutrients hosts relatively diverse cryptogamic dry tundra

dominated by bryophytes mainly *Polytrichum juniperinum* Hedw. and *P. piliferum* Hedw. mixed with lichen *Ochrolechia frigida* (Sw.) Lynge and scattered tussocks of two angiosperms: *D. antarctica* and *Colobanthus quitensis* (Kunth) Bartl. Tundra communities developed near the northern coast are dominated by two flowering plants: *D. antarctica* and *C. quitensis*, which can form (especially *D. antarctica*) dense patches. The identification of tundra community was based on direct ground observation conducted in 2008/2009 summer season where five dominated tundra communities were identified and mapped. However, photointerpretation of our UAV images allowed the identification of only four types of communities. Exposed and very dry sites were habitats of fruticose lichens mainly *Usnea antarctica* (Du Rietz) and *U. aurantiaco-atra* (Jacq.), but the lichen covered surfaces were impossible to be mapped on the UAV images.

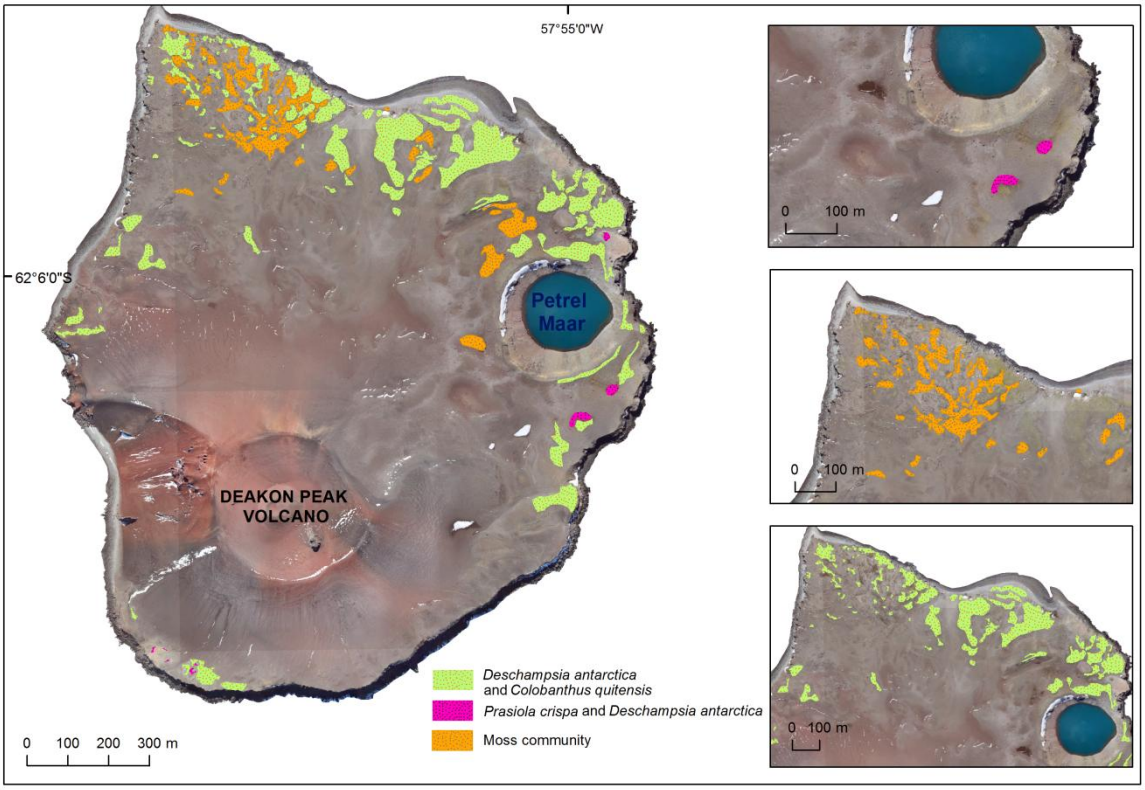

Fig. 7. Map of vegetation on Penguin Island, based on UAV images (vectorised in ESRI ArcGIS).

4.3. Landforms

We were able to map 10 landforms of volcanic origin, 3 of mass movement landforms, 5 fluvial, 1 aeolian, and 3 coastal landforms. Additionally, all snow patches, a lake and other surfaces of not recognized origin were distinguished (Fig. 8).

The Deakon Peak crater is about 360 m wide and hosts secondary landforms such as the central cone with its little crater. A small volcanic plug and several small residual ridges constituting outcrops of the Deakon Peak Formation (DPF) are visible inside the crater and were mapped previously (Birkenmajer 1979, 1982; Pańczyk and Nawrocki, 2011). The western flank of the stratovolcano is modified by a landslide which produced a large scar and excavated numerous small ridges of the DPF (Fig. 4, 8). The landslide was probably triggered by the eruption of a submarine maar immediately west of the stratovolcano (Birkenmajer, 1979, 1982). The eastern rim of the principal cone is depressed and the slope below shows signs of mass movement which ended close to the SW side of the Petrel maar. We interpreted this as a scoria flow which occurred after 1979 AD, because it is absent on the sketch map of Birkenmajer (1979, 1982). The minimum age of the flow is also unknown because later publications (Pańczyk and Nawrocki, 2011; Angiel and Dąbski, 2012) duplicated the abovementioned map of Birkenmajer (with minor modifications) and show no scoria flow. It is, therefore, possible that the landform is very recent.

Erosional furrows developed in the lower parts of the principal cone, especially on its northern slopes, and they were not depicted on any previously published map. They sometimes evolve into episodic river channels lined with the system of fluvial landforms, abundant in the northern part of the island.

Close to the foothills of the SE flank of the stratovolcano, there is a field of small arched landforms indicating slow downlope movement, and interpreted by us as creep terraces.

These landforms were not mapped previously, presumably because they constitute only a minor modification of outer slopes of the volcano.

Immediately south of the terraces, at the volcano foothills, there is a little field with little light-yellow ridges orientated parallel to each other which we interpret as dunes. Similar landforms were found around a little pond located within the reach of the scoria flow. These, presumably aeolian landforms were not depicted on former maps (Birkenmajer 1979, 1982; Pańczyk and Nawrocki, 2011).

The Petrel maar crater, with a similar diameter to that of the principal cone, has steep internal slopes with outcrops of rocks belonging to the Marr Point Formation (Birkenmajer, 1979). A lake, 18 m deep, fills the bottom and serves as climate change record since Medieval Period (Wasiłowska et al., 2017). Numerous volcanic bombs can be seen around the flanks of the maar testifying for a violent eruption of the maar, possible between 1500BP and 1250BP (Wasiłowska et al., 2017). Our orthophoto and DEM did not allow us to map the extend of the maar flanks, visible on the map of Birenmajer (1979, 1982), because the slopes are too gentle. However, unlike former studies, we were able to map numerous outcrops of the Marr Point Formation rocks. They occur alternately with a system of shallow dry valleys, remodeled by rain and melt waters which drain into straight or braided river channels developed on valley floors.

Around the island, there is a system of raised marine terraces (Birkenmajer, 1979) but we were unable to clearly vectorise them on UAV images. However, active coastal landforms such as beaches and cliffs, in places modeled by rockfalls, were detected. Beaches are best developed along the northern coast, where the mean altitude of island surface is not significant. Cliffs are typical for the southern coast and indicate that the base of the Petrel Maar and the Decon Peak stratovolcato is currently subject to intensive lithoral erosion.

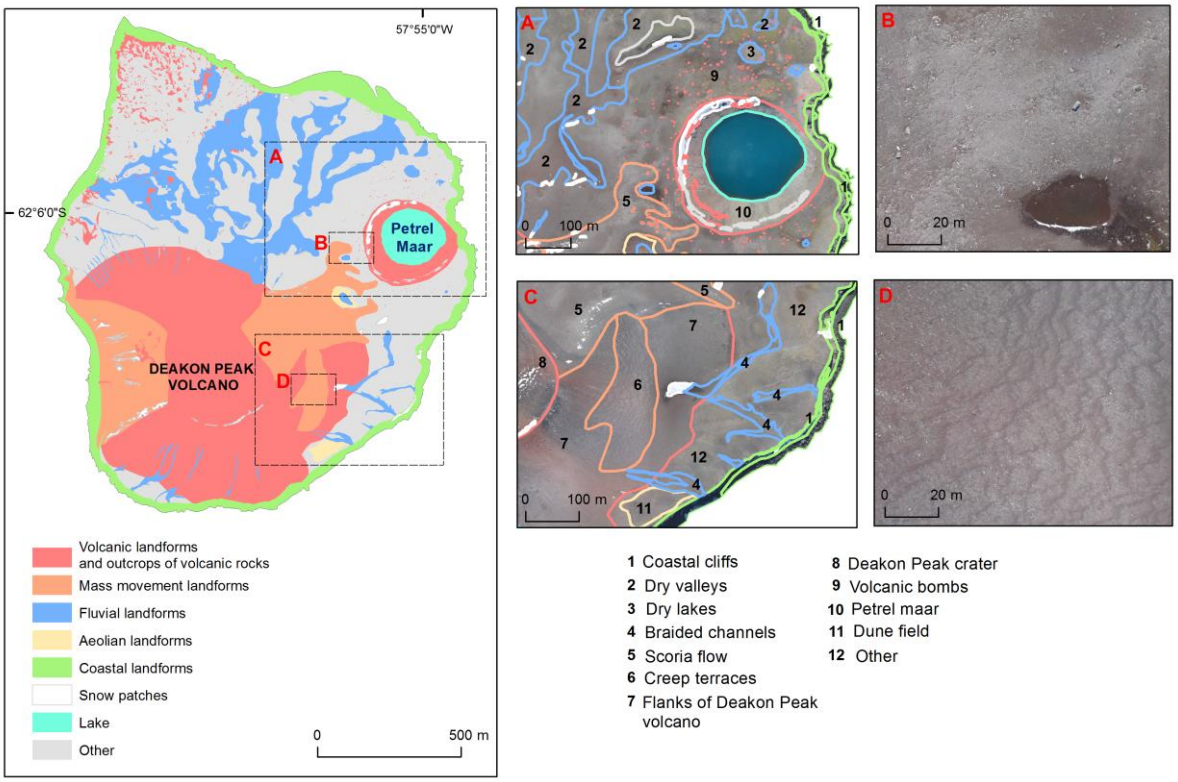

Fig. 8. Landforms of Penguin Island, based on UAV images (vectorised in ESRI ArcGIS). Image B shows a marginal part of a scoria flow, a dry lake and a few volcanic bombs, image D shows creep terraces developed on flanks of Deakon Peak volcano.

5. Discussion

The mission to collect multidisciplinary data in Antarctic conditions during the fixed-wing UAV BVLOS operation was successful. It demonstrated that high-quality data could be gathered from distant and isolated areas. A traditional survey on Penguin Island requires more than two hours of one way trip by a dinghy at open sea (minimum two boats for safety reasons) from Arctowski, and a couple of fieldwork days. Under harsh, rapidly changing weather conditions typical for the maritime Antarctic (Kejna et al., 2013), this kind of mission is very difficult, risky and time-consuming. Our previous study already showed that the use of PW-ZOOM UAV in this region seems to be much more efficient in comparison with traditional observation in the field (Dąbski et al. 2017) or even with other remote sensing

techniques, like e.g. satellite (Mustafa et al. 2012). However, to reach the target located 30 km from Arctowski, the mission required the BVLOS flight.

5.1. Previous Antarctic UAV BVLOS operations

In Antarctica, there were just a few examples of successful uses of fix wing UAV in BVLOS operations. First time in 2007, a mini-UAV M2AV developed by the British Antarctic Survey and the University of Braunschweig (Germany) was used for meteorological research at Halley Station, South Weddell Sea (Sanderson, 2008; Spiess et al., 2007). In 2008/2009, ship-based observations of free-drifting icebergs were supported by two models of UAVs (Plane-Sig Kadet Senior and Sig Rascal 110), which were launched from a ship (McGill et al., 2011). In 2009, Aerosonde UAVs were used in Terra Nova Bay (Ross Sea) to study the interaction of katabatic winds and sea ice formation (Cassano et al., 2010). Subsequent successful flights were conducted between Livingston Island and Deception Island (South Shetlands) in December 2011 by Ant-plane 3 and Ant-plane 6 specially designed for Antarctic conditions. This mission provided aeromagnetic and aerial photographic data from the northern part of Deception Island (Funaki et al., 2013, 2014). In 2013/2104, GIX UAS performed first radar measurements of ice thickness of a fast-moving glacier with fine resolution to determine glacier bed topography and basal conditions over subglacial Whillans Lake and the WISSARD drill site in the central Antarctic (Leuschen et al., 2014).

5.2. Monitoring of Antarctic fauna: opportunities and limitations

The use of UAVs to monitor the fauna in the Antarctic region seems highly efficient in comparison with other remote techniques, such as satellite imaging. Moreover, satellite imaging of breeding colonies to estimate the number of nests encounters difficulties (LaRue et al., 2014), including optimal terrain resolution parameters (e.g. medium-resolution Landsat-

7 imagery 30 m pixel size; VHR satellite imagery ~0.60 m pixel size) (Lynch and Schwaller, 2014). Obtaining good-quality material from satellites at an appropriate time may be difficult due to the specificity of the climate in this region, characterized by frequent occurrences of dense cloud cover and mist (Mustafa et al., 2012). Observations must be carried out at a strictly specified moment of the breeding chronology when animals are concentrated on the land. The dates of task-flights must be synchronized with the breeding chronology of each animal species under investigation (CCAMLR 2014). The limited time (e.g. approx. two weeks in the case of the breeding birds) to obtain proper aerial data also significantly increases the probability that extreme weather conditions will arise, which in turn considerably increases the risk that the whole mission will fail. Also, in the case of some species of penguin breeding together in the same colony, it is only possible to identify the total number of nests on UAV images (GDS: 0.07 m), and it is impossible to subdivide them into individual species. We noted this problem in the case of Adélie and chinstrap penguins mixed in the same breeding groups. The body sizes and the distances between the nests for both species are similar (see above chapter Results), so additional reference data from the ground level is needed. This problem does not exist in the case of other species like gentoo penguins, because the spatial pattern of their nests is significantly different from the other *Pygoscelis* species (Müller-Schwarze and Müller-Schwarze, 1975; Volkman and Trivelpiece, 1981). Previous own study of UAV derived material (Zmarz et al. 2015) allowed to identify a strict differences in the distribution pattern of gentoo individuals incubating eggs within breeding group, comparing to the remaining two species. Such a characteristic was clearly visible and here is presented on Fig 6. According to Pfeiffer and Peter (2004) eleven bird species nest on Penguin Island, including nine flying marine birds, e.g. southern giant petrel (*Macronectes giganteus*) or south polar skua (*Stercorarius maccormicki*). However, no other species of birds were identified on UAV images, except for two penguin species. Taking into

account the body size, breeding chronology and specific nesting preferences, of all the flying bird species listed by Pfeiffer and Peter (2004) only the southern giant petrel (body size 85-100 cm) could be identified on the analyzed photogrammetric material (GSD 0.07 m). Lack of identified southern giant petrel breeding sites on orthophoto were noticed. The reason of that could be an indistinguishable color of bird plumage on the rock background.

The example of implementation of APQ-18 quadrocopters and APH-22 hexacopter to investigate Antarctic pinniped populations was reported by Goebel et al. (2015) and Krause et al (2017). Images obtained from the very low altitude (up to 45 m, 0.01-0.03 m GRD) were successfully used for estimation of the number (Goebel et al., 2015), the mass and the body conditions (Krause et al., 2017) of fur seal and leopard seal species. According to our experience, identification of pinniped species in the UAVs images with a resolution of 0.07 m is also feasible and relatively effortless, because species characteristic pelage patterns and colors are clearly visible. Moreover, the average size of the bodies (e.g. the southern elephant seal: male 4.5-6.5 m, female 2.5-4.0 m, pup 1.3 m; Weddell seal: male 2.5-3.0 m, female 2.6-3.3 m, pup 1.2-1.5 m) is sufficient to be detected as a distinctive feature.

UAVs with electric engines are reportedly less noisy than UAVs with combustion ones and when flying at 350 m AGL they cause practically no impact on the animals being monitored (Korczak-Abshire et al., 2016). However, potential influence on wildlife in the case of UAVs with combustion engines is very little (Korczak-Abshire et al., 2016), especially when compared with ground methods, or with multicopter UAVs which usually operate at much lower altitudes (Vas et al., 2015; Rümmler et al., 2016; Braun et al., 2014) than UAVs.

5.3. Mapping vegetation

It is extremely difficult to map Antarctic vegetation due to the very high spatial variability induced by the complex morphology of the terrain (Dąbski et al., 2017), patchy and

mosaic character of microhabitats, extremely differentiated by abiotic features, e.g. water conditions, salinity and the nutrient content of the substratum (Nędzarek et al., 2014). This patchiness shapes the distribution of organisms and – combined with harsh climate conditions – causes poor development and loose vegetation cover (Chwedorzewska and Bednarek, 2008). Specific features of Antarctic vegetation distribution make even very high spatial resolution satellite imagery (pixel size of 0.5 m) unsuitable for mapping tundra extent in sufficient detail (Farwell et al., 2011; Lucieer et al., 2014). Thus, one of the key requirements for mapping the Antarctic vegetation distribution is the acquisition of ultra-high spatial resolution imagery, e.g. 0.01 m pixel size or better, in order to capture the fine-scale spatial variability of tundra communities. Remote sensing imagery for mapping vegetation with ground-truth validation in Antarctica (and sub-Antarctic) is still in the trial stage. Some few exceptions are based on medium resolution imagery from Landsat on the Antarctic Peninsula (Fretwell et al., 2011), from SPOT in the Kerguelen archipelago (Robin et al., 2011) and also based on very high resolution image datasets from IKONOS on Heard Island (Murray et al., 2010) and Terra Nova Bay (Kim and Hong, 2012). Therefore, detail data on Antarctic vegetation are sparse and limited to easily accessible areas located mainly in the vicinity of research stations and based largely on traditional field study (Calviño-Cancela and Martín-Herrero, 2016). Using UAVs opens up new possibilities for mapping vegetation in very specific Antarctic conditions (Anderson and Gaston, 2013; Berni et al., 2009), especially in the Antarctic, where field studies employing the classic method of vegetation mapping are limited due to inaccessibility and scattering of ice-free areas. Moreover, the Antarctic tundra is very fragile and in some areas like e.g. wet moss-bed, any direct human impact can leave footprints for years (Chwedorzewska and Korczak, 2010). Small multicopters were already successfully used to collect visible, multispectral and thermal images of moss-beds, providing the non-invasive method to measure changes in their micro-topography (Lucieer et al., 2014) and physiological

state (Turner et al., 2014). Different types of cyanobacterial mats were identified and mapped in McMurdo Dry Valleys with a small fixed-wing UAV (Bollard-Breen et al., 2015). Thus, UAV-based remote sensing methods, represent an alternative for field study, allowing the survey of a broad area and reducing the perturbations derived from observers. Furthermore, the data obtained from UAV can be easily integrated into a geographic information system (GIS) and can constitute the basis for future broad analyses of environmental changes. Due to the patchy nature of the Antarctic tundra, dominated by cryptogams: lichens, mosses, algae, with only two native flowering plants (Ochyra, 1998; Ochyra et al., 2008; Olech, 2002, 2004), interspersed with bare ground, and the similarity between the species, the UAV collected data must be supported by ground direct observation or hyperspectral remote sensing (Black et al., 2014; Shin et al., 2014; Vieira et al., 2014). Especially in the areas where communities are dominated by lichens this technique can fail and might lead to serious underestimation of vegetation cover area (Casanovas et al., 2015).

5.4. Mapping landforms

Very high spatial resolution of the images obtained allowed us to precisely map the landforms whose origin raised no doubts. However, there are significant areas of the island not recognized in terms of morphogenesis, which were named “other surfaces” (Fig. 6). They probably constitute lava flows covered by weathering mantle or fine-grained pyroclastic material. Only drilling or excavation would reveal structure and texture of the sediments and bedrock, and therefore provide evidence of the origin of the landforms. UAV imaging solely based on visual light is insufficient for full geomorphological mapping, nevertheless, it allows for precise determining of the spatial extent of typical, easy-to-recognize landforms. One of the greatest advantages of UAV geomorphological mapping is the fast execution rate and easy access to remote and desolate areas.

Hackney and Clayton (2015) emphasize advantages of UAVs platforms (fixed-wing and rotor-wing) and SfM photogrammetric technique in geomorphological studies, because they provide data of large spatial scales and high temporal resolution. The UAVs are increasingly used in a variety of geomorphological research, including studies of: river channels (Flener et al., 2007), erosion gullies (d'Oleire-Oltmanns et al. 2012; Grellier et al. 2012), debris flows and alluvial fans (de Haas et al. 2014), landslides (Niethammer et al. 2012), glacial landforms (Whitehead et al. 2013, Chandler et al. 2016), karstic landscape (Silva et al. 2017) or in structural geomorphology (Kasprzak et al. 2017). However, none of these studies utilized the BVLOS operations and all required physical presence of the researcher in or very close to the study site. The advantage and novelty of our operation was that it allowed us to picture remote and difficult-to-access landforms in the polar environment, located 30 km away from the operating team.

5.5. Safety regulations

The extreme meteorological condition and rugged terrain encountered in Antarctica present risks in the operation of UAV. There is legitimate concern that UAVs may pose a danger to the safety of people and infrastructure, especially in areas such as KGI, with multiple scientific stations with expanded facility belonging to different parties, an airstrip (Chilean Presidente Eduardo Frei Montalva Base) forming the transportation hub of KGI, and considerable air and marine tourist traffic constraints. Thus, there is a probability of unanticipated events like unplanned landings, aircraft loss, collisions with other airspace users or with infrastructure. But on the other hand, deployment of UAV to gather environmental data can significantly reduce the direct human impact on the objects monitored (e.g. by disturbing animals or trampling tundra) (Braun et al., 2014) and would provide less invasive methods of environmental data collection. The quick development in UAV-based

environmental data acquisition in Antarctica has outpaced our ability to assess its impact on wildlife and calls for regulatory guidelines. To address these issues, the authors initiated a monitoring program aimed at measuring the potential effects of UAV disturbance, first on breeding Adélie penguins (Korczak-Abshire et al., 2016), and later on gentoo penguins (*Pygoscelis papua*) and southern giant petrels. At the same time, the authors cooperated with the Antarctic Treaty Consultative Meetings/Committee for Environmental Protection (ATCM/CEP) on formulating safety protocols which were successfully used by us during the consecutive Antarctic field seasons (Poland, Government 2015, 2016, 2017a and 2017b). This subject is nowadays one of the priorities discussed during the ATCM to develop guidelines and Standard Operating Procedures that will enable safe and responsible used of this technology. Presently, the Council of Managers of National Antarctic Program (COMNAP) in cooperation with ATCM/CEP formed the basis of Handbook that should be viewed as a living document which, as UAV technology evolves, finds a new application. This Handbook will be reviewed at least twice a year to ensure safety of any other airspace users and of ground personnel, natural environment (especially area of ASPAs), infrastructure and equipment. Hazards and risks should be identified and assessed for each specific deployment as for any airborne object, advance notification and communications with other operators in any given region is essential to reduce the risk of harm (COMNAP RPAS 2017).

6. Conclusions

The BVLOS operation of fixed-wing PW-ZOOM UAV, equipped with a visual light camera and performed in harsh Antarctic conditions, allowed us to obtain high-quality photogrammetric material for monitoring the key elements of a polar ecosystem of Penguin Island. After their transformation into orthophoto and processing in GIS, the images obtained allowed us to produce precise maps of fauna, flora, and landforms and to collect quantitative

environmental data. The images obtained permitted to map the sites occupied by Adélie and chinstrap penguins, southern elephant and Weddell seals, and three types of tundra communities. Numerous landforms of volcanic, mass movement, fluvial, coastal and aeolian origin were mapped.

We conclude that the use of UAV BVLOS operations improves environmental monitoring in polar regions by: extending the study area, increasing safety, reducing human footprints, increasing precision, and saving time. These are the features which permit repetitive observations of a variety of distant and hard-to-access areas which nowadays undergo environmental modifications due to climatic changes.

Acknowledgement

The research was conducted as part of the project "A novel approach to monitoring the impact of climate change on Antarctic ecosystems (MONICA)" funded by the Polish-Norwegian Research Programme operated by the National Centre for Research and Development under the Norwegian Financial Mechanism 2009-2014 in the frame of Project Contract No. 197810. Gracious thanks are directed to dr Anna Kidawa for help in preparing permit documentation to conduct research on KGI, Adam Tomaszewski and Paweł Kusideł for UAV operating and service, and all the other members involved in the implementation of MONICA project for their various and complex support. The data used in the paper were collected at the Henryk Arctowski Polish Antarctic Station. The authors thank the editor and anonymous reviewers for constructive comments on the original version of the article.

References

Ancel, A., Cristofari, R., Fretwell, P.T., Trathan, P.N., Wienecke, B., 2014. Emperors in hiding: when ice-breakers and satellites complement each other in Antarctic exploration. PLoS ONE 9, e100404. doi: 10.1371/journal.pone.0100404.

Anderson, K., Gaston, K.J., 2013. Lightweight unmanned aerial vehicles will revolutionize spatial ecology. Front. Ecol. Environ. 11 (3), 138–146. doi:10.1890/120150.

Androsiuk, P., Chwedorzewska, K.J., Szandar, K., Giełwanowska, I., 2015. Genetic variation of the *Colobanthus quitensis* from King George Island (Antarctica). Pol. Polar Res. 36, 281–295. doi : 10.1515/popore−2015−0017.

Angiel, P.J., Dąbski, M., 2012. Lichenometric ages of the Little Ice Age moraines on King George Island and of the last volcanic activity on Penguin Island (West Antarctica). Geogr. Ann. Series A, Phys. Geogr. 94, 395–412. doi: 10.1111/j.1468-0459.2012.00460.x.

Barber-Meyer, S.M., Kooyman, G.L., Ponganis, P.J., 2007. Estimating the relative abundance of emperor penguins at inaccessible colonies using satellite imagery. Polar Biol. 30, 1565–1570. doi: 10.1007/s00300-007-0317-8.

Berni, J., Zarco-Tejada, P., Suarez, L., Fererez, E., 2009. Thermal and narrow-band multispectral remote sensing for vegetation monitoring from an unmanned aerial vehicle. IEEE T Geosc. Remote 47 (3), 722–738. doi: 10.1109/TGRS.2008.2010457.

Birkenmajer, K., 1979. Age of the Penguin Island Volcano, South Shetland Islands (West Antarctica), by the Lichenometric Method. Bull. Aced. Pol. Sci-Earth 27 (1-2), 69–76.

Birkenmajer, K., 1982. The Penguin Island volcano, South Shetland Islands (Antarctica): its structure and succession. Stud. Geol. Pol. 74, 155–173.

Black, M., Casanovas, P., Convey, P., Fretwell, P., 2014. High resolution mapping of Antarctic vegetation communities using airborne hyperspectral data. RSPSoc 2014, 2-5th September 2014, Aberystwyth, UK. doi: 10.13140/2.1.5189.6648.

Bollard-Breen, B., Brooks, J. D., Jones, M. R. L., Robertson, J., Betschart, S., Kung, O., Craig Cary, S., Lee, C.K., Pointing, S.B., 2015. Application of an unmanned aerial vehicle in spatial mapping of terrestrial biology and human disturbance in the McMurdo Dry Valleys, East Antarctica. Polar Biol. 38, 573–578. doi: 10.1007/s00300-014-1586-7.

Black, M., Casanovas, P., Convey, P., Fretwell, P., 2014. High resolution mapping of Antarctic vegetation communities using airborne hyperspectral data. RSPSoc 2014, 2-5th September 2014, Aberystwyth, UK. doi: 10.13140/2.1.5189.6648.

Braun, C., Hertel, F., Mustafa, O., Nordt, A., Pfeiffer, S., Peter, H-U. 2014. Environmental assessment and management challenges of the Fildes Peninsula Region. Tin T. et al., (eds.), In: Antarctic Futures, 169-191. doi: 10.1007/978-94-007-6582-5_7.

Braun, C., Mustafa, O., Nordt A., Pfeiffer S., Peter, H-U., 2012. Environmental monitoring and management proposals for the Fildes Region, King George Island, Antarctica. Polar Res. 31, 18206. doi: 10.3402/polar.v31i0.18206.

Calviño-Cancela, M., Martín-Herrero, J., 2016. Spectral discrimination of vegetation classes in ice-free areas of Antarctica. Remote Sens. 8, 856. doi: 10.3390/rs8100856.

Casanovas, P., Black. M., Fretwell, P., Convey, P., 2015. Mapping lichen distribution on the Antarctic Peninsula using remote sensing, lichen spectra and photographic documentation by citizen scientists. Polar Res. 34, 25633. doi: 10.3402/polar.v34.25633.

Cassano, J., Maslanik, J.A., Zappa, C.J., Gordon, A.L., Cullather, R.I., Knuth, S.L., 2010. Observations of Antarctic polynya. EOSTrans. Am. Geophysical Union 91, 245–246. doi: 10.1029/2010EO280001.

CCAMLR, 2014, CCAMLR Ecosystem Monitoring Program Standard Methods, https://www.ccamlr.org/en/system/files/CEMP%20Standard%20Methods%20Jun%202014.pdf.

659 Chamaille-Jammes, S., Guinet, C., Nicoleau, F., Argentier, M.A., 2000. A method to assess
660 population changes in king penguins: The use of a Geographical Information System to
661 estimate area-population relationships. Polar Biol. 23, 545–549. doi: 10.1007/s003000000119
662 Chandler, B.M.P., Evans, D.J.A., Roberts, D.H., Ewertowski, M., Clayton, A. I., 2016.
663 Glacial geomorphology of the Skálafellsjökull foreland, Iceland: A case study of 'annual'
664 moraines, J. Maps 12 (5), 904–916. doi: 10.1080/17445647.2015.1096216.
665 Christie, K.S., Gilbert, S.L., Brown, C.L., Hatfield, M., Hanson, L., 2016. Unmanned aircraft
666 systems in wildlife research: current and future applications of a transformative technology.
667 Front. Ecol. Envir 14(5), 241–251. doi: 10.1002/fee.1281.
668 Chwedorzewska, K.J., 2009. Terrestrial Antarctic Ecosystems at the Changing World – an
669 overview. Pol. Polar Res. 30 (3), 263–273. doi: 10.4202/ppres.2009.13.
670 Chwedorzewska, K.J., Bednarek, P.T., 2008. Genetic variability in the Antarctic hairgrass
671 *Deschampsia antarctica* Desv. from maritime Antarctic and sub-Antarctic sites. Pol. J. Ecol.
672 56, 209–216.
673 Chwedorzewska, K.J., Korczak, M, 2010. Human impact upon the environment in the vicinity
674 of *Arctowski* Station, King George Island, Antarctica. Pol. Polar Res. 31, 45–60. doi:
675 10.4202/ppres.2010.04.
676 COMNAP RPAS Working Group 2017. Antarctic Remotely Piloted Aircraft Systems (RPAS)
677 Operator's Handbook. Information Paper 050, XL ATCM held in Beijing, China, 22 May
678 2017 - 01 Jun 2017.
679 Convey, P., Chown, S.L., Clarke, A., Barnes, D.K.A., Bokhorst, S., Cummings, V., Ducklow,
680 H.W., Frati, F., Green, T.G.A., Gordon, S., Griffiths, H.J., Howard-Williams, C., Huiskes,
681 A.H.L., Laybourn-Parry, J., Lyons, W.B., McMinn, A., Morley, S.A., Peck, L.S., Quesada, A.,
682 Robinson, S.A., Schiaparelli, S., Wall, D.H., 2014. The spatial structure of Antarctic
683 biodiversity. Ecol. Monogr. 84, 203–244. doi: 10.1890/12-2216.1.

Dąbski, M., Zmarz, A., Pabjanek, P., Korczak-Abshire, M., Karsznia, I., Chwedorzewska, K., 2017. UAV-Based detection and spatial analyses of periglacial landforms on Demay Point (King George Island, South Shetland Islands, Antarctica). Geomorphology 290, 29–38. doi: 10.1016/j.geomorph.2017.03.033.

de Haas, T., Ventra, D., Carbonneau, P.E., Kleinhans, M.G., 2014. Debris-flow dominance of alluvial fans masked by runoff reworking and weathering. Geomorphology 217, 165–181. doi: 10.1016/j.geomorph.2014.04.028.

d'Oleire-Oltmanns. S, Marzolff, I., Peter, K.D., Ries, J.B., 2012. Unmanned Aerial Vehicle (UAV) for Monitoring Soil Erosion in Morocco. Remote Sens. 4, 3390–3416. doi: 10.3390/rs4113390.

Flener, C., Lotsari, E., Alho, P., Käyhkö, J.,. 2012. Comparison of empirical and theoretical remote sensing based bathymetry models in river environments. River Res. App. 28 (1), 118–133. doi: 10.1002/rra.1441.

Fretwell, P.T., Convey, P., Fleming, A.H., Peat, H.J., Hughes, K.A., 2011. Detecting and mapping vegetation distribution on the Antarctic Peninsula from remote sensing data. Polar Biol. 34, 273–281. doi: 10.1007/s00300-010-0880-2.

Fretwell, P.T., LaRue, M.A., Morin, P., Kooyman, G.L., Wienecke, B., et al., 2012. An Emperor Penguin Population Estimate: The First Global, Synoptic Survey of a Species from Space. PLoS ONE 7(4): e33751. doi: 10.1371/journal.pone.0033751.

Fretwell, P.T., Phillips, R.A., de L. Brooke, M., Fleming, A.H., McArthur, A., 2015. Using the unique spectral signature of guano to identify unknown seabird colonies. Remote Sens. Envir. 156, 448–456. doi: 10.1016/j.rse.2014.10.011.

Fretwell, P.T., Trathan, P.N., 2009. Penguins from space: Faecal stains reveal the location of emperor penguin colonies. Glob. Ecol. Biogeogr. 18, 543–552. doi: 10.1111/j.1466-8238.2009.00467.x.

709 Funaki, M., Higashino, S.I., Sakanaka, S., Iwata, N., Nakamura, N., Hirasawa, N., Obara, N.,
710 Kuwabara, M., 2014. Small unmanned aerial vehicles for aeromagnetic surveys and their
711 flights in the South Shetland Islands, Antarctica. Polar Sci. 8, 342–356. doi:
712 10.1016/j.polar.2014.07.001.
713 Funaki, M., Higashino, S.I., Sakanaka, S., Iwata, N., Nakamura, N., Hirasawa, N., Obara. N.,
714 Kuwabara, M., 2013. Aeromagnetic and aerial photographic survey in the South Shetland
715 Islands, Antarctica, conducted by a small unmanned aerial vehicle (Ant-Plane). Antarctic Rec.
716 57, 209–214. doi: 10.1016/j.polar.2014.07.001.
717 Goebel, M.E., Perryman, W.L., Hinke, J.T., Krause, D.J., Hann, N.A., Gardner, S., LeRoi,
718 D.J., 2015. A small unmanned aerial system for estimating abundance and size of Antarctic
719 predators. Polar Biol. 38, 619–630. doi: 10.1007/s00300-014-1625-4.
720 Goetzendorf-Grabowski, T., Rodzewicz, M., 2017. Design of UAV for photogrammetric
721 mission in Antarctic area. Challenges in European Aerospace. P I Mech Eng G-J Aer. doi:
722 10.1177/0954410016656881.
723 Grellier, S., Kemp, J., Janeau, J.J., Florsch, N., Ward, D., Barot, S., Podwojewski, P., Lorentz,
724 S., Valentin, C., 2012. The indirect impact of encroaching trees on gully extension: A 64 year
725 study in a sub-humid grassland of South Africa. Catena 98, 110–119. doi:
726 10.1016/j.catena.2012.07.002.
727 Gugliemin, M., 2012. Advances in permafrost and periglacial research in Antarctica: a review.
728 Geomorphology 155-156, 1–6. doi: 10.1016/j.geomorph.2011.12.008.
729 Hackney, C., Clayton, A., 2015. Unmanned Aerial Vehicles (UAVs) and their application in
730 geomorphic mapping. In: Clarke, L., Nield, J. M. (Eds.) Geomorphological Techniques. London,
731 GB, British Soc. Geomorph. Retrieved from: http://eprints.soton.ac.uk/id/eprint/376639.

Harris, C.M., 2005. Aircraft operations near concentrations of birds in Antarctica: The development of practical guidelines. Biol. Conserv. 125, 309–322. doi: 10.1016/j.biocon.2005.04.002.

Harris, C.M., Lorenz, K., Fishpool, L.D.C., Lascelles, B., Cooper, J., Coria, N.R., Croxall, J.P., Emmerson, L.M., Fraser, W.R., Fijn, R.C., Jouventin, P., LaRue, M.A., Le Maho, Y., Lynch, H.J., Naveen, R., Patterson-Fraser, D.L., Peter, H.U., Poncet, S., Phillips, R.A., Southwell, C.J., van Franeker, J.A., Weimerskirch, H., Wienecke, B., Woehler, E.J., 2015. Important bird areas in Antarctica 2015. BirdLife Int. and Environ. Res. & Assessment Ltd., Cambridge.

Hodgson, J.C., Baylis, S.M., Mott, R., Herrod, A., Clarke, R.H., 2016. Precision wildlife monitoring using unmanned aerial vehicles. Sci. Rep. 6, 22574. doi: 10.1038/srep22574.

Hughes, K.A., Waluda, C.M., Stone, R.E., Ridout, M.S., Shears, J.R., 2008. Short-term responses of king penguins *Aptenodytes patagonicus* to helicopter disturbance at South Georgia. Polar Biol. 31, 1521–1530. doi: 10.1007/s00300-008-0492-2.

Jabłoński, B., 1980. Distribution and numbers of birds and pinnipeds on Penguin Island (South Shetland Islands) in January 1979. Pol. Polar Res. 1, 109–116.

Jabłoński, B., 1984. Distribution and numbers of penguins in the region of King George Island (South Shetland Islands) in the breeding season 1980/1981, Pol. Polar Res. 5, 17–30.

Kasprzak, M., Jancewic, K., Michniewicz, A., 2017. UAV and SfM in Detailed Geomorphological Mapping of Granite Tors: An Example of Starościńskie Skały (Sudetes, SW Poland). Pure Appl. Geophys. 1–15. doi: 10.1007/s00024-017-1730-8.

Kejna, M., Araźny, A., Sobota, I., 2013. Climatic change on King George Island in the years 1948–2011. Pol. Polar Res. 34, 213–235. doi: 10.2478/popore-2013-0004.

Kim, S.U., Hong, C.H., 2012. Antarctic land-cover classification using IKONOS and Hyperion data at Terra Nova Bay. Int. J. Rem. Sens. 33, 7151–7164. doi: 10.1080/01431161.2012.700136.

Korczak-Abshire, M., Chwedorzewska, K.J., Wąsowicz, P., Bednarek, P.T., 2012. Genetic structure of declining chinstrap penguin (*Pygoscelis antarctica*) populations from South Shetland Islands (Antarctica). Polar Biol. 35, 1681–1689. doi: 10.1007/s00300-012-1210-7.

Korczak-Abshire, M., Kidawa, A., Zmarz, A., Storvold, R., Karlsen, S.R., Rodzewicz, M., Chwedorzewska, K., Znój, A., 2016 Preliminary study on nesting Adélie penguins disturbance by unmanned aerial vehicles. CCAMLR Sci. 23,1–16.

Krause, D.J., Hinke, J.T., Perryman, W.L., Goebel, M.E., LeRoi, D.J., 2017. An accurate and adaptable photogrammetric approach for estimating the mass and body condition of pinnipeds using an unmanned aerial system. PLoS ONE 12(11): e0187465. doi: 10.1371/journal.pone.0187465.

LaRue, M.A., Lynch, H. J., Lyver, P.O.B., Barton, K., Ainley, D.G., Pollard, A., Fraser, W.R., Ballard, G., 2014. A method for estimating colony sizes of Adélie penguins using remote sensing imagery. Polar Biol. 37 (4), 507–517. doi: 10.1007/s00300-014-1451-8.

Leuschen, C., Hale, R., Keshmiri, S., Yan, J., Rodriguez-Morales, F., Mahmood, A., Gogineni, S., 2014. UAS-based radar sounding of the polar ice sheets. IEEE Geosc. Rem. Sens. Mag 2, 8–17. doi: 10.1109/MGRS.2014.2306353.

López-Martínez, J., Serrano, E., Schmid, T., Mink, S., Linés, C., 2012. Periglacial processes and landforms in the South Shetland Islands (northern Antarctic Peninsula region). Geomorphology 155-156, 62–79. doi: 10.1016/j.geomorph.2011.12.018.

Lucieer, A., Turner, D., King, D.H., Robinson, S.A., 2014. Using an Unamanned Aerial Vehicle (UAV) to capture micro-topography of Antarctic moss beds. Inter. J. Appl. Earth. Observ. Geoinfo. 27, 53–62. doi: 10.1016/j.jag.2013.05.011.

Lynch, H.J., Schwaller, M.R., 2014 Mapping the Abundance and Distribution of Adélie Penguins Using Landsat-7: First Steps towards an Integrated Multi-Sensor Pipeline for Tracking Populations at the Continental Scale. PLoS ONE 9 (11), e113301. doi: 10.1371/journal.pone.0113301.

McGill, P.R., Reisenbichler, K.R., Etchemendy, S.A., Dawe, T.C., Hobson, B.W., 2011. Aerial surveys and tagging of freedrifting icebergs using an unmanned aerial vehicle (UAV). Deep-Sea Res Pt II, 58, 1318–1326. doi: 10.1016/j.dsr2.2010.11.007.

McMahon, C.R., Howe, H., van den Hoff, J., Alderman, R., Brolsma, H., Hindell, M.A., 2014. Satellites, the all-seeing eyes in the sky: counting elephant seals from space. PLoS ONE 9 (3), e92613. doi: 10.1371/journal.pone.0092613.

Murray, H., Lucieer, A., Williams, R., 2010. Texture-based classification of sub-Antarctic vegetation communities on Heard Island. Inter. J. App. Earth Observ. Geoinfo. 12, 138–149. doi: 10.1016/j.jag.2010.01.006.

Mustafa, O., Esefeld, J., Grämer, H., Maercker, J., Rümmler, M.C., Senf, M., Pfeifer, C., Peter, H.U., 2017. Monitoring penguin colonies in the Antarctic using remote sensing data. Final Report. Project Environmental Research of the Federal Ministry for the Environment, Nature Conservation, Building and Nuclear Safety. Retrieved from: https://www.umweltbundesamt.de/en/publikationen/monitoring-penguin-colonies-in-the-antarctic-using.

Mustafa, O., Pfeifer, C., Peter, H., Kopp, M., Metzig, R., 2012. Pilot Study on Monitoring Climate-Induced Changes in Penguin Colonies in the Antarctic Using Satellite Images; German Ministry of the Federal Environment: Dessau-Roßlau, Germany.

Müller-Schwarze, C., Müller-Schwarze, D., 1975. A survey of twenty-four rook- eries of pygoscelid penguins in the Antarctic Peninsula region. Pp. 309–320 In: Stonehouse, B., (Ed.)The biology of penguins. University Park Press, London, England.

805 Naveen, R., Forrest, S.C., Dagit, R.G., Blight, L.K., Trivelpiece, W.Z., Trivelpiece, S.G.,
806 2000. Censuses of penguin, blue-eyed shag and southern giant petrel populations in the
807 Antarctic Peninsula region, 1994–2000. Polar Rec. 36, 323–334. doi:
808 10.1017/S0032247400016818.
809 Nędzarek, A., Tórz, A., Drost, A. 2014. Selected elements in surface waters of Antarctica and
810 their relations with the natural environment. Polar Res. 33, 21417. doi:
811 10.3402/polar.v33.21417.
812 Niethammer, U., James, M.R., Rothmund, S., Travelletti, J., Joswig, M., 2012. UAV-based
813 remote sensing of the Super-Sauze landslide: Evaluation and results. Engin. Geol. 128, 2–11.
814 doi: 10.1016/j.enggeo.2011.03.012.
815 Ochyra, R. 1998. The moss flora of King George Island Antarctica. Polish Academy of
816 Science. Szafer Institute of Botany, Cracow, 278 pp.
817 Ochyra, R., Lewis-Smith, L.R.I., Bednarek−Ochyra, H., 2008. The illustrated moss flora of
818 Antarctica. Cambridge University Press, Cambridge, 685 pp.
819 Olech, M., 2002. Plant communities on King George Island. In*:* Beyer, L., Bölter, M. (Eds.)
820 Geoecology of Antarctic Ice−free coastal landscapes. Ecol. Stud. 154, 215–231.
821 Olech, M., 2004. Lichens of King George Island Antarctica. The Institute of Botany of the
822 Jagiellonian University, Cracow, 391 pp.
823 Pańczyk, M., Nawrocki, J., 2011. Pliocene age of the oldest rocks of Penguin Island (South
824 Shetlands, northern Antarctic Peninsula). Geol. Quart. 55 (4), 335–344.
825 Pfeiffer, S., Peter, H.U., 2004. Ecological studies toward the management of an Antarctic
826 tourist landing site (Penguin Island, South Shetland Islands). Polar Rec. 40, 1–9. doi:
827 10.1017/S0032247404003845.

828 Pfeiffer, S., Braun, C., Mustafa, O., Peter, H.U., 2007. Tourism Growth and Proposed
829 Management Solutions in the Fildes Peninsula Region (King George Island, Antarctica).
830 Tourism in Marine Environ. 4, 151–165. doi: 10.3727/154427307784771995.
831 Poland, Government of. 2015. UAV remote sensing of environmental changes on King
832 George Island (South Shetland Islands): preliminary information on the results of the first
833 field season 2014/2015. Information Paper 077, XXXVIII ATCM held in Sofia, Bulgaria, 01-
834 10 Jun 2015.
835 Poland, Government of. 2016. UAV remote sensing of environmental changes on King
836 George Island (South Sheltland Islands): update on the results of the second field season
837 2015/2016. Information Paper 059, XXXVIII ATCM held in Santiago, Chile, 23 May 2016 -
838 01 Jun 2016.
839 Poland, Government of. 2017a. UAV remote sensing of environmental changes on King
840 George Island (South SHeltland Islands): update on the results of the third field season
841 2016/2017. Information Paper 045, XL ATCM held in Beijing, China, 22 May 2017 - 01 Jun
842 2017.
843 Poland, Government of. 2017b. UAV impact – problem of a safe distance from wildlife
844 concentrations. Information Paper 046, XL ATCM held in Beijing, China, 22 May 2017 - 01
845 Jun 2017.
846 Pudełko, R., Angiel, P.J., Potocki, M., Jędrejek, A., Kozak, M., 2018. Fluctuation of Glacial
847 Retreat Rates in the Eastern Part of Warszawa Icefield, King George Island, Antarctica,
848 1979–2018. Remote Sens. 10, 892. doi:10.3390/rs10060892.
849 Rakusa-Suszczewski, S., 2002. King George Island – South Shetland Islands, Maritime
850 Antarctic. In: Beyer, L., Bölter M. (Eds.) Geoecology of Antarctic Ice-Free Coastal
851 Landscapes. Springer, pp. 427. doi: 10.1007/978-3-642-56318-8.

852 Rakusa-Suszczewski, S., Nędzarek, A., 2002. Whale bones and macroalgae as source of
853 nutrients and cations in the nearshore geoecosystem of Admiralty Bay (King George Island,
854 Antarctica). Pol. J. Ecol. 50 (3), 389–396.
855 Robin, M., Chapuis, J.L., Lebouvier, M., 2011. Remote sensing of vegetation cover change in
856 islands of the Kerguelen archipelago Polar Biol. 34, 1689–1700. doi: 10.1007/s00300-011-
857 1069-z.
858 Rodzewicz, M., Głowacki, D., Hajduk, J., 2017. Some dynamic aspects of photogrammetry
859 missions performed by "PW-ZOOM" – the UAV of Warsaw University of Technology. Arch.
860 Mech. Eng. 64 (1), 37–55. doi: 10.1515/meceng-2017-0003.
861 Rümmler, M.C., Mustafa, O., Maercker, J., Peter, H.U., Esefeld, J., 2016. Measuring the
862 influence of unmanned aerial vehicles on Adélie penguins. Polar Biol. 39 (7), 1329–1334. doi:
863 10.1007/s00300-015-1838-1.
864 Salwicka, K., Rakusa-Suszczewski, S., 2002. Long-term monitoring of Antarctic pinnipeds in
865 Admiralty Bay (South Shetlands, Antarctica). Acta Theriol. 47, 443–457. doi:
866 10.1007/BF03192469.
867 Sander, M., Coelho Balbão, T., Schneider Costa, E., dos Santos., R.C., Petry, M.V., 2007.
868 Decline of the breeding population of *Pygoscelis antarctica* and *Pygoscelis adeliae* on
869 Penguin Island, South Shetland, Antarctica. Polar Biol. 30, 651–654. doi: 10.1007/s00300-
870 006-0218-2.
871 Sangra, P., Gordo, C., Hernandez-Arencibia, M., Marrero-Diaz, A., Rodrıguez-Santana, A.,
872 Stegner, A., Martinez-Marrero, A., Pelegrıd, J-L, Pichon, T., 2011. The Bransfield current
873 system. Deep-Sea Res. 58 (4), 390–402. doi: 10.1016/j.dsr.2011.01.011.
874 Schmid, T., Guillaso, S., López-Martínez, J., Nieto, A., Mink, S., Koch, M., D'Hondt, O.,
875 Maestro, A., Serrano, E., 2016. Mapping ice-free areas of King George Island (South
876 Shetland Islands, Antarctica) using full polarimetric RADARSAT-2 data. In: Günther, F.,

877 Morgenster, A. (Eds.), XI. International Conference on Permafrost, Potsdam, Germany, pp.
878 141.
879 Schwaller, M.R., Southwell, C.J., Emmerson, L.M., 2013. Continental-scale mapping of
880 Adélie penguin colonies from Landsat imagery. Remote Sens. Environ. 139, 353–364. doi:
881 10.1016/j.rse.2013.08.009.
882 Shin, J.I., Kim, H.C., Kim, S.I., Hong, S.G., 2014. Vegetation abundance on the Barton
883 Peninsula, Antarctica: estimation from high-resolution satellite images. Polar Biol. 37, 1579–
884 1588. doi: 10.1007/s00300-014-1543-5.
885 Sierakowski, K., Korczak-Abshire, M., Jadwiszczak, P., 2017. Changes in bird communities
886 of Admiralty Bay, King George Island (West Antarctica): insights from monitoring data
887 (1977-1996). Pol. Polar Res. 38 (2), 231–262. doi: 10.1515/popore-2017-0010.
888 Silva, O.L., Bezerra, F.H.R., Maia, R.P., Cazarin, C.L., 2017. Karst landforms revealed at
889 various scales using LiDAR and UAV in semi-arid Brazil: Consideration on karstification
890 processes and methodological constraints. Geomorphology 295, 611–630. doi:
891 10.1016/j.geomorph.2017.07.025.
892 Schwaller, M.R., Southwell, C.J., Emmerson, L.M., 2013. Continental-scale mapping of
893 Adélie penguin colonies from Landsat imagery. Remote Sens. Environ. 139, 353–364. doi:
894 10.1016/j.rse.2013.08.009.
895 Shin, J.I., Kim, H.C., Kim, S.I., Hong, S.G., 2014. Vegetation abundance on the Barton
896 Peninsula, Antarctica: estimation from high-resolution satellite images. Polar Biol. 37, 1579–
897 1588. doi: 10.1007/s00300-014-1543-5.
898 Shirihai , H. (Ill. by B. Jarrett), 2002. A complete guide to Antarctic wildlife: the birds and
899 marine mammals of the Antarctic continent and the Southern Ocean. Princeton University
900 Press.

Southwell, C., Emmerson, L., 2013. Large-scale occupancy surveys in East Antarctica discover new Adélie penguin breeding sites and reveal an expanding breeding distribution. Antarctic Sci. 25 (4), 531–535. doi: 10.1017/S0954102012001174.

Southwell, C., McKinlay, J., Low, M., Wilson, D., Newbery, K., Lieser, J.L., Emmerson, L., 2013. New methods and technologies for regional-scale abundance estimation of land-breeding marine animals: application to Adélie penguin populations in East Antarctica. Polar Biol. 36 (6), 843–856. doi: 10.1007/s00300-013-1310-z.

Terauds, A., Chown, S.L., Morgan, F., Peat, J., Watts, H., Keys, D.J., Convey, P., Bergstrom, D.M., 2012. Conservation biogeography of the Antarctic. Divers Distrib. 18, 726–741. doi: 10.1111/j.1472-4642.2012.00925.x.

Trathan, P.N., 2004. Image analysis of color aerial photography to estimate penguin population size. Wildl. Soc. Bull. 32, 332–343. http://www.jstor.org/stable/3784973.

Trivelpiece, W.Z., Trivelpiece, S.G., Volkman, N.J., 1987. Ecological segregation of adelie, gentoo and chinstrap penguins at King George Island, Antarctic Ecol. 58 (2), 351–361. doi: 10.2307/1939266.

Turner, J., Bindschadler, R., Convey, P., di Prisco, G., Fahrbach, E., Gutt, J., Hodgson, D., Mayewski, P., Summerhayes, C., 2009. Antarctic Climate Change and the Environment; Scientific Committee on Antarctic Research: Cambridge, UK.

Turner, D., Lucieer, A., Malenovský, Z., King, D.H., Robinson, S.A., 2014. Spatial Co-Registration of Ultra-High Resolution visible, multispectral and thermal images acquired with a Micro-UAV over Antarctic moss beds. Rem. Sens. 6, 4003–4024. doi:10.3390/rs6054003.

Vas, E., Lescroël, A., Duriez, O., Boguszewski, G., Grémillet, D., 2015. Approaching birds with drones: first experiments and ethical guidelines. Biol. Lett. 11, 20140754. doi: http://dx.doi.org/10.1098/rsbl.2014.0754.

925 Vieira, G., Mora, C., Pina, P., Schaefer, C.E.R., 2014. A proxy for snow cover and winter
926 ground surface cooling: Mapping Usnea sp. communities using high resolution remote
927 sensing imagery (Maritime Antarctica). Geomorphology 225, 69–75. doi:
928 10.1016/j.geomorph.2014.03.049.
929 Volkman, N.J., Trivelpiece, W., 1981. Nest-Site Selection among Adélie, Chinstrap and
930 Gentoo Penguins in Mixed Species Rookeries. Wilson Bull. 93, 243–248.
931 http://www.jstor.org/stable/4161463.
932 Wasiłowska, A., Tatur, A., Pushina, Z., Barczuk, A., Verkulich, S., 2017. Impact of the 'Little
933 Ice Age' climate cooling on the maar lake ecosystem affected by penguins: A lacustrine
934 sediment record, Penguin Island, West Antarctica. Holocene 27 (8), 1115 – 1131. doi:
935 10.1177/0959683616683254.
936 Watts, A.C., Ambrosia, V.G., Hinkley, E.A., 2012. Unmanned Aircraft Systems in Remote
937 Sensing and Scientific Research: Classification and Considerations of Use. Rem. Sens. 4,
938 1671–1692. doi: 10.3390/rs4061671.
939 Whitehead, K., Moorman, B.J., Hugenholtz, C.H., 2013. Brief communication: Low-cost, on-
940 demand aerial photogrammetry for glaciological measurement. Cryosphere 7, 1879–1884. doi:
941 10.5194/tc-7-1879-2013.
942 Witharana, C., Lynch, H. J., 2016. An Object-Based Image Analysis Approach for Detecting
943 Penguin Guano in very High Spatial Resolution Satellite Images. Rem. Sens. 8 (5), 375.
944 doi:10.3390/rs8050375.
945 Zhou, G., 2009. Near Real-Time orthorectification and mosaic of small UAV video flow for
946 time-critical event response. IEEE T Geosci. Remote 47 (3), 739–747. doi:
947 10.1109/TGRS.2008.2006505.
948 Znój, A., Chwedorzewska, K. J., Androsiuk, P., Cuba-Diaz, M., Giełwanowska, I., Koc, J.,
949 Zmarz, A., 2017. Rapid environmental changes in the Western Antarctic Peninsula region due

950 to climatechange and human activity. App. Ecol. Envir. Res. 15, 525–539. doi:
951 10.15666/aeer/1504_525539.
952 Zmarz, A., Korczak-Abshire, M., Storvold, R., Rodzewicz, M., Kędzierska, I., 2015. Indicator
953 species population monitoring in Antarctica with UAV. The International Archives of the
954 Photogrammetry, Remote Sensing and Spatial Information Sciences XL-1/W4.
955 doi.org/10.5194/isprsarchives-XL-1-W4-189-2015.
956 Zhou, G., 2009. Near Real-Time orthorectification and mosaic of small UAV video flow for
957 time-critical event response. IEEE T Geosci. Remote 47 (3), 739–747. doi:
958 10.1109/TGRS.2008.2006505.
959 Zwoliński, Z., 2007. Mobilność materii mineralnej na obszarach paraglacjalnych, Wyspa
960 Króla Jerzego, Antarktyka Zachodnia [The mobility of mineral matter in paraglacial area,
961 King George Island, Western Antarctica - in Polish]. In: Seria Geograficzna. 74 Adam
962 Mickiewicz University Press, Poznań, 266 pp.